Enabling the Optimisation of the Primary Suspension with Passive Components for an Industrial Railway Vehicle Model

T. Lewis [1], **Y. Li** [1], **J. Jiang** [1], **S. Neild** [1], **G. Tucker** [2], **S. Iwnicki** [2], **R. Goodall** [2], **M. Smith** [3]
[1] Department of Mechanical Engineering, University of Bristol,
Queen's Building, University Walk, Bristol, BS8 1TR, UK
e-mail: **tl1485@bristol.ac.uk**

[2] Institute of Railway Research, University of Huddersfield,
Queensgate, Huddersfield, HD1 3DH, UK

[3] Department of Engineering, University of Cambridge,
Trumpington Street, Cambridge, CB2 1PZ, UK

Abstract
The use of inerters in the lateral suspension of railway vehicles has been proven, in recent studies using lumped mass models, to provide benefits in terms of track wear and passenger comfort improvement. Validation of these enhancements using an industry standard simulation tool, which analyses realistic vehicle models with numerous degrees of freedom, is essential if the railway industry is going to adopt this new piece of technology. The problems associated with this, however, come in the form of large complicated numerical matrices, slow inversion times, and algebraic loops associated with the inerter's acceleration dependence. The systematic investigation of candidate vibration absorber configurations is also problematic. To this end, this paper proposes a Location Matrix method of simulation which enables the optimisation of interchangeable suspension networks within large dynamic systems by the use of a Laplace to state-space transformation. This method, which can be applied to any dynamic system and needs only the knowledge of the base mass, stiffness and damping matrices, is validated using a low degree of freedom system, and it is found that for railway vehicles, optimisation on a linearised or semi-linearised model can be performed. Nonlinearities arising from the varying contact patch normal force mean that further investigation is needed before a full analysis can take place.

1 Introduction

Passive suspensions can be characterised using networks comprising springs, dampers and inerters, which, via the mechanical to electrical force-current analogy, relate respectively to inductors, resistors and capacitors. An inerter [1] is a two-terminal mechanical suspension element which generates a force proportional to the relative acceleration between its terminals. First introduced into Formula 1 under the pseudonym *J-Damper* [2], the inerter enables mechanical networks to simulate any passive response. Research into their vibration suppression benefits is rich, and comes in the fields of road vehicles [3–5], buildings [6–8] and optical tables [9], amongst others. Conventional passive railway vehicle suspensions make use of springs and dampers to suppress unwanted vibrations. Active methods of suppressing railway vehicle vibration have been successfully studied in [10–12]; however problems relating to measurement error, fault tolerances, actuator malfunction and torque requirements are increasingly making passive control with the addition of inerters more appealing. The implementation of inerters in railway vehicle suspension systems has been investigated, in previous numerical studies using lumped mass models [13–15], and they have been found to

be beneficial in terms of improving ride comfort and curving performance.

Research into the use of inerters using the modelling software, VAMPIRE® , is ongoing [16] with the aim of reinforcing the findings reported using lumped mass models. VAMPIRE® is a widely used industry standard simulation tool, which provides the means to model railway vehicles more realistically and in greater detail. Simply adding an inerter in parallel to an existing suspension does not necessarily provide the desired benefits. To fully investigate the benefits of inerter-based suspension networks it is necessary to first explore all, or as many as possible spring/damper/inerter networks and identify the optimum network with an optimum set of element parameters. This is difficult to achieve in VAMPIRE® as the simulations would be computationally intensive and the software does not lend itself to the systematic investigation of a wide range of absorber configurations. The matrices defining the Equations of Motion (EOMs) of the system can be exported from VAMPIRE® ; however, for a full vehicle model they are large, and it can be difficult to identify the physical meaning of every matrix entry such that they can be modified to accommodate different device dynamics during an optimisation procedure. This problem is compounded if additional degrees of freedom are present in the suspension. To this end, this paper establishes an approach named the Location Matrix method, with the aim of enabling the optimisation of primary suspension vibration suppression devices with any number of internal states, using exported numerical matrices from VAMPIRE® .

The method proposed in this paper provides the user with a time domain analysis simulation tool within which Laplace admittance functions of suspension networks of any complexity can be varied accordingly. It is applicable to any dynamic system and eliminates SIMULINK® errors occurring as a result of algebraic loops when the inerter is modelled in parallel due to its acceleration dependence. It reduces the simulation time considerably when the number of Degrees of Freedom (DOFs) is large, due to the increased complexity of matrix inversions, and importantly can be used on systems where only the numerical rather than algebraic mass, stiffness and damping matrices of the base system without the vibration suppression device are known. The structure of this paper is as follows: Section 2 introduces the generalised Location Matrix method in detail, whilst Section 3 validates it using a simple MATLAB® model. Section 4 discusses the extent to which it can be applied to railway vehicles, and overall conclusions are drawn in Section 5.

2 The Location Matrix Method of Dynamic System Modelling

The following is a derivation of the method conceived to transform the EOM of a generalised n-DOF dynamic system, which includes an optimisable suspension network $Y(s)$, from Laplace to state-space form. Consider the following Laplace EOM:

$$s^2 M_0 \tilde{\underline{x}} + sC_0 \tilde{\underline{x}} + K_0 \tilde{\underline{x}} + sY(s) L_m \tilde{\underline{x}} = B \tilde{\underline{u}}. \tag{1}$$

where M_0 is the mass matrix, $Y(s)$ is the admittance function of the suspension network under investigation, L_m is the Location Matrix which identifies coupling locations and coefficients corresponding to the addition to the model of the $Y(s)$ suspension network, while C_0 and K_0 are respectively the damping and stiffness matrices for the rest of the system. $\underline{x}$ is the state matrix, $\underline{u}$ is the input matrix, with inputs denoted by B, s is the Laplace variable, $\tilde{\underline{x}}$ is the Laplace transform of $\underline{x}$ and $\tilde{\underline{u}}$ the Laplace transform of $\underline{u}$.

If the term $sY(s)L_m\tilde{\underline{x}}$ is ignored, Equation 1 describes the base model without the inclusion of the suspension network, $Y(s)$. If there are m identical copies of the $Y(s)$ suspension network in various locations within the model, the symmetric Location Matrix, L_m, can be written in the form VV^T where $V \in \mathbb{R}^{\mathrm{n}\times\mathrm{m}}$. The i^{th} column of V, where $i = 1 \ldots m$, identifies the parameters and coupling positions which are required to correctly alter the EOMs of the overall system when the i^{th} $Y(s)$ suspension network is included in the model. It hence follows that:

$$sV_i^T \tilde{\underline{x}} = \Delta v_i \tag{2}$$

where Δv_i is the relative change in velocity between the DOFs associated with the i^{th} device. The force to acceleration transfer function of the $Y(s)$ suspension network can be written as,

$$Y'(s) = \frac{Y(s)}{s} = \frac{F_i}{\Delta a_i}, \tag{3}$$

where F_i is the force exerted on the i^{th} device and Δa_i is the associated relative change in acceleration at the i^{th} device. $Y'(s)$ must be positive-real [17]; I.E $|\alpha - \phi| \leq 1$ where α and ϕ denote respectively the highest powers of s on the numerator and denominator of $Y'(s)$.

$$Y'(s) = \frac{\beta_0 s^p + \beta_1 s^{p-1} + \cdots + \beta_{p-1} s + \beta_p}{s^p + \alpha_1 s^{p-1} + \cdots + \alpha_{p-1} s + \alpha_p}. \tag{4}$$

The following equations show the result of the transformation of the now positive semi-definite function $Y'(s)$ into state-space form, using one example of the non-unique canonical decomposition technique.

$$Y'(s) = c_1(sI - A_1)^{-1} b_1 + d_1 \tag{5}$$

$$A_1 = \begin{bmatrix} 0 & 1 & 0 & \dots & 0 \\ 0 & 0 & 1 & \dots & 0 \\ \vdots & \vdots & \vdots & \ddots & \vdots \\ 0 & 0 & 0 & \dots & 1 \\ -\alpha_p & -\alpha_{p-1} & -\alpha_{p-2} & \dots & -\alpha_1 \end{bmatrix} \tag{6}$$

$$b_1 = \begin{bmatrix} 0_{p\times 1} \\ 1 \end{bmatrix} \tag{7}$$

$$c_1 = \begin{bmatrix} (\beta_p - \alpha_p\beta) & (\beta_{p-1} - \alpha_{p-1}\beta) & \dots & (\beta_2 - \alpha_2\beta) & (\beta_1 - \alpha_1\beta) \end{bmatrix} \tag{8}$$

$$d_1 = \beta_0 \tag{9}$$

It is possible to obtain L_m for large industrial systems using reverse engineering and analysing a range of MCK matrices with differing suspension parameters. However, it is extremely difficult to interpret these matrices and decompose L_m into the VV^T format, due to lack of algebraic information, the large numbers of DOFs and hence a very complicated and varied set of couplings for each $Y(s)$ network. It has been found that the decomposition of L_m is not unique and there exists more solutions in the form of UU^T. Equating VV^T and a discovered UU^T, it can be shown that $V = UQ$ where $Q = U^T V^{-T}$, $QQ^T = I$, and hence $V_i^T = Q^T U_i^T$. Substituting $V = UQ$ into Equation 2,

$$sQ^T U_i^T \underline{\tilde{x}} = \Delta v_i \tag{10}$$

and multiplying by Q^{-T},

$$sU_i^T \underline{\tilde{x}} = \Delta v_{fi} \tag{11}$$

a fictitious set of states is introduced, denoted by the subscript f. The following equations show how the now fictitious forces (F_{fi}) and accelerations (a_{fi}) relate to the physical system:

$$F_{fi} = QF_i \tag{12}$$

$$Y'(s) = \frac{F_i}{\Delta a_i} = \frac{F_{fi}}{\Delta a_{fi}} \tag{13}$$

The derivation of the state-space simulation method begins with $L_m = UU^T$ and hence adjoins fictitious states w_f, with the use of fictitious accelerations a_f. If the input to $Y'(s)$ for the i^{th} fictitious suspension network location is the change in relative fictitious accelerations of various system DOFs, ${U_i}^T \underline{x} s^2$, then r copies of the state Y' can be adjoined as follows, where $F_{{Y'}_{fi}}$ are the fictitious $Y'(s)$ suspension forces at the i^{th} fictitious suspension network location,

$$\underline{\dot{w}}_{f1} = A_1 \underline{w}_{f1} + b_1 {U_1}^T \underline{\tilde{x}} s^2, \tag{14}$$

$$F_{{Y'}_{f1}} = c_1 \underline{w}_{f1} + d_1 {U_1}^T \underline{\tilde{x}} s^2, \tag{15}$$

to

$$\underline{\dot{w}}_{fr} = A_1 \underline{w}_{fr} + b_1 {U_r}^T \underline{\tilde{x}} s^2, \tag{16}$$

$$F_{{Y'}_{fr}} = c_1 \underline{w}_{fr} + d_1 {U_r}^T \underline{\tilde{x}} s^2. \tag{17}$$

Let $\underline{z}$ be the forces provided by $Y(s)$:

$$\underline{z} = Y'(s) L_m \underline{\tilde{x}} s^2 = UY'(s)U^T \underline{\tilde{x}} s^2 = (U_1 Y'(s) {U_1}^T + U_2 Y'(s) {U_2}^T + ... + U_r Y'(s) {U_r}^T) \underline{\tilde{x}} s^2. \tag{18}$$

$Y'(s){U_i}^T \underline{\tilde{x}} s^2$ describes the i^{th} set of fictitious $Y'(s)$ forces as defined in Equation 17. Therefore, making suitable substitutions, Equation 18 can be written as,

$$\underline{z} = U_1(c_1 \underline{w}_{f1} + d_1 {U_1}^T \underline{\tilde{x}} s^2) + U_2(c_1 \underline{w}_{f2} + d_1 {U_2}^T \underline{\tilde{x}} s^2).... + U_r(c_1 \underline{w}_{fr} + d_1 {U_r}^T \underline{\tilde{x}} s^2). \tag{19}$$

Equation 1 can now be modified to include $\underline{z}$, defining the suspension forces provided by the $Y(s)$ device,

$$M_0 \underline{\tilde{x}} s^2 + C_0 \underline{\tilde{x}} s + K_0 \underline{\tilde{x}} + \underline{z} = B \underline{\tilde{u}}. \tag{20}$$

Multiplying by s, substituting in Equation 19 for $\underline{z}$, and hence introducing the $Y'(s)$ states $\underline{\dot{w}}_{f1}, \ldots, \underline{\dot{w}}_{fr}$,

$$M_0 \underline{\tilde{x}} s^3 + C_0 \underline{\tilde{x}} s^2 + K_0 \underline{\tilde{x}} s + \sum_{i=1}^{r} U_i (c_1 \underline{\dot{w}}_{fi} + d_1 U_i^T \underline{\tilde{x}} s^3) = B \underline{\tilde{u}} s, \tag{21}$$

Substituting for $\underline{\dot{w}}_{fi}$ using Equation 16, a new system EOM can be formed:

$$M_0\tilde{\underline{x}}s^3 \;+\; C_0\tilde{\underline{x}}s^2 \;+\; K_0\tilde{\underline{x}}s \;+\; \sum_{i=1}^{r} U_i(c_1(A_1\underline{w}_{fi} \;+\; b_1{U_i}^T\tilde{\underline{x}}s^2) \;+\; d_1U_i^T\tilde{\underline{x}}s^3) \quad = \quad B\tilde{\underline{u}}s. \tag{22}$$

Grouping powers of s, and performing the reverse substitutions:

$$M_0' = M_0 + \sum_{i=1}^{r} U_i d_1 U_i^T, \tag{23}$$

$$C_0' = C_0 + \sum_{i=1}^{r} U_i c_1 b_1 U_i^T, \tag{24}$$

a generalised and simplified EOM can be formed:

$$M_0'\tilde{\underline{x}}s^3 + C_0'\tilde{\underline{x}}s^2 + K_0\tilde{\underline{x}}s + \sum_{i=1}^{r} U_i(c_1A_1\dot{\underline{w}}_{fi}) = B\tilde{\underline{u}}s. \tag{25}$$

The entire system can now be written in the time domain, in state-space form, with the fictitious states $\underline{w}_{fi}$ adjoined as follows:

$$\frac{d}{dt}\begin{bmatrix} \ddot{\underline{x}} \\ \dot{\underline{x}} \\ \underline{x} \\ \underline{w}_{fi} \\ \vdots \\ \underline{w}_{fr} \end{bmatrix} = A_{ss}\begin{bmatrix} \ddot{\underline{x}} \\ \dot{\underline{x}} \\ \underline{x} \\ \underline{w}_{fi} \\ \vdots \\ \underline{w}_{fr} \end{bmatrix} + B_{ss}\dot{\underline{u}} \tag{26}$$

$$A_{ss} = \begin{bmatrix} -{M_0'}^{-1}C_0' & -{M_0'}^{-1}K_0 & 0 & -{M_0'}^{-1}U_1c_1A_1 & \dots & -{M_0'}^{-1}U_rc_1A_1 \\ I & 0 & 0 & 0 & \dots & 0 \\ 0 & I & 0 & 0 & \dots & 0 \\ b_1{U_1}^T & 0 & 0 & A_1 & \dots & 0 \\ \vdots & \vdots & \vdots & \vdots & \ddots & 0 \\ b_1{U_r}^T & 0 & 0 & 0 & 0 & A_1 \end{bmatrix} \tag{27}$$

$$B_{ss} = \begin{bmatrix} {M_0'}^{-1}B \\ 0_{(2n+r)\times 1} \end{bmatrix} \tag{28}$$

A more visually understandable realisation of Equation 26 is described below, where the deletion of the state $\underline{x}$ results in the deletion of the third row and column of A_{ss}, forming A_{ss}', (a similar manipulation to B_{ss} occurs) and Equation 26 is integrated with respect to time.

$$\dot{X} = {A_{ss}}'X + {B_{ss}}'\underline{u} \tag{29}$$

$$X = \begin{bmatrix} \dot{\underline{x}} & \underline{x} & \int \underline{w}_{fi} & \dots & \int \underline{w}_{fr} \end{bmatrix}' \tag{30}$$

$$A_{ss}{}' = \begin{bmatrix} -{M_0'}^{-1}C_0' & -{M_0'}^{-1}K_0 & -{M_0'}^{-1}U_1c_1A_1 & \dots & -{M_0'}^{-1}U_rc_1A_1 \\ I & 0 & 0 & \dots & 0 \\ {b_1U_1}^T & 0 & A_1 & \dots & 0 \\ \vdots & \vdots & \vdots & \ddots & 0 \\ {b_1U_r}^T & 0 & 0 & 0 & A_1 \end{bmatrix} \tag{31}$$

$$B_{ss}{}' = \begin{bmatrix} {M_0'}^{-1}B \\ 0_{(n+r)\times 1} \end{bmatrix} \tag{32}$$

3 Validation of the Location Matrix Method Using a Low-Order Model in MATLAB®

Before testing this method on an industrial railway vehicle model, it is necessary to validate it using a simpler system. The system chosen is a standard two-mass oscillator, shown in Figure 1, and contains a direct $Y(s)$ connection between the two masses. Figure 2 shows the six candidate $Y(s)$ networks, and Table 1 denotes the values of all the parameters used. The initial validation uses the true Location Matrix,

$$L_m = \begin{bmatrix} 1 & -1 \\ -1 & 1 \end{bmatrix} \tag{33}$$

and compares the responses of mass 1 to input forces F_{s1} and F_{s2} on masses 1 and 2 respectively, using the L1 version of $Y(s)$, calculated three ways:

- **Tfsys A**. The standard formation of the Laplace EOMs, incorporating $Y(s)$ into the system matrix manually.
- **Tfsys Lm**. A slight variation of Tfsys A in which a Location Matrix is used in conjunction with the base mass, damping and stiffness matrices of the system.
- **YsLm SS**. The fully automated Location Matrix method, using the L_m decomposition, laid out in Section 2.

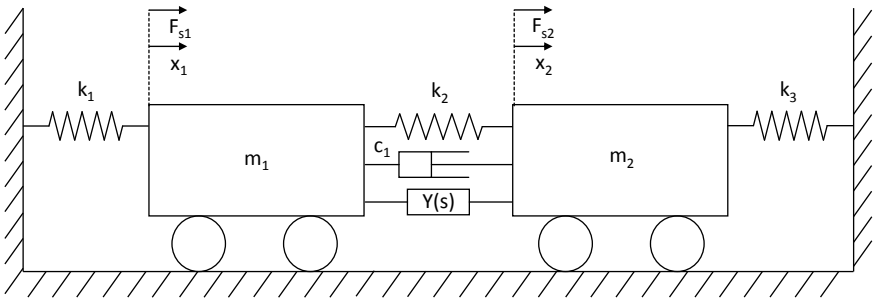

Figure 1: The two-mass oscillator used to test the Location Matrix theory in MATLAB®

The forces F_{s1} and F_{s2} can be either harmonic or step in nature, as detailed in Figure 3.

Parameter	Value	Unit
m_1	1250	kg
m_2	3000	kg
k_1	8×10^5	N/m
k_2	9×10^5	N/m
k_3	6.8×10^5	N/m
c_1	6.3×10^4	Ns/m
k_y	2.55×10^5	N/m
k_s	2.99×10^5	N/m
c_s	5.20×10^4	Ns/m
b_s	6.67×10^3	kg
b_{s2}	4×10^3	kg

Table 1: The values of the masses and components of Figure 1, along with the fixed values of the $Y(s)$ network components from Figure 2

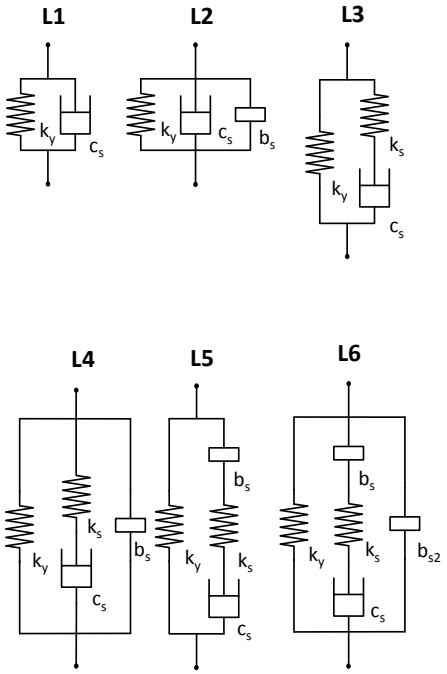

Figure 2: The $Y(s)$ networks

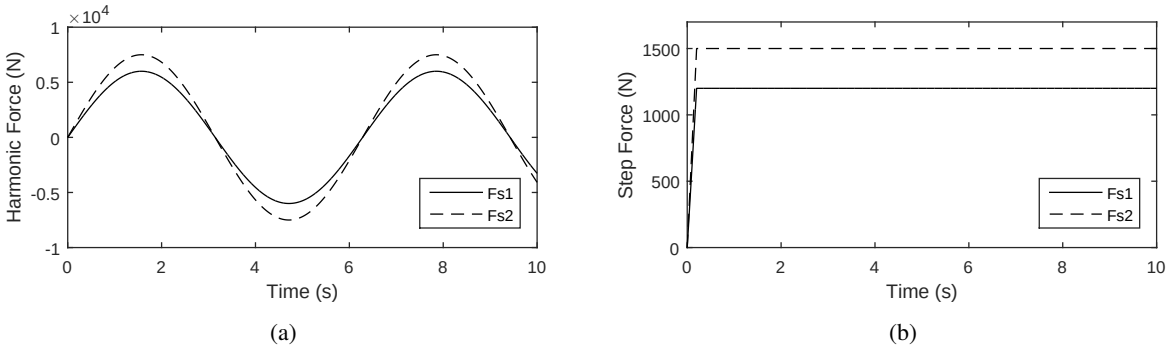

(a) (b)

Figure 3: The input forces at mass 1 (F_{s1}) and mass 2 (F_{s2}), for the harmonic and step input cases.

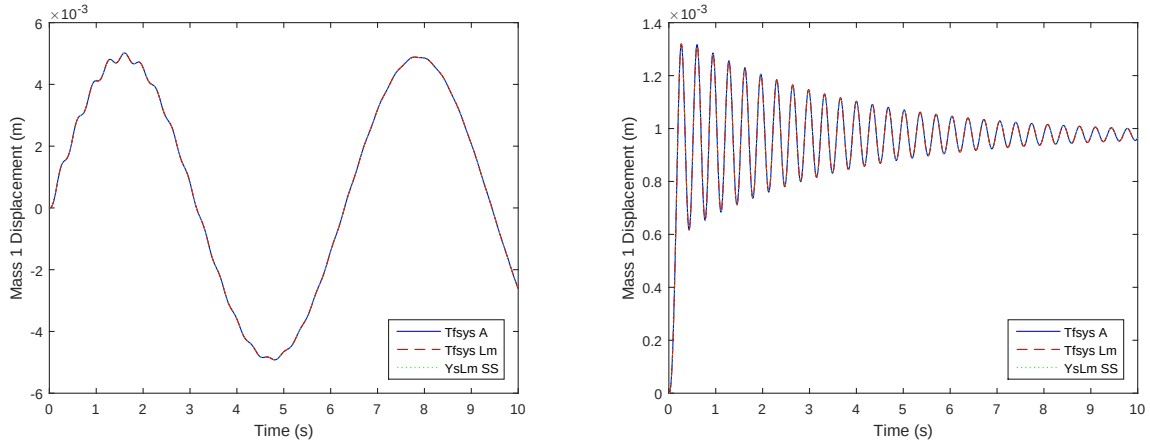

(a) (b)

Figure 4: A comparison between the three methods of simulating the simple dynamic system, with the original location matrix, in response to the harmonic input (a), and the step input (b) at mass 1, using an L1 $Y(s)$ layout

Figure 4 shows the matching responses using the three methods described above, and therefore confidence can be gained in the Location Matrix method analysis technique. The next step in the validation procedure is to test a number of different Location Matrices and different $Y(s)$ layouts. Firstly, returning to the notation used in Section 2, two different V matrices are arbitrarily defined as:

$$V_1 = \begin{bmatrix} 1 \\ -1 \end{bmatrix} \tag{34}$$

$$V_2 = \begin{bmatrix} 1 & 1 & 5 \\ -1 & -34.6 & 0 \end{bmatrix} \tag{35}$$

These The fact that V_2 has no physical meaning in conjunction with Figure 1 is not important as it is the theoretical method that is being tested here. These two V matrices correspond to test cases 1 and 2. The two corresponding Location Matrices can be formed using VV^T to ensure their symmetricity, and hence two decompositions into UU^T can be performed, each in two ways:

- Single Value Decomposition (SVD). This produces a diagonal matrix s, and unitary matrices U_s and V_s, such that $U_s V_s$ = I and $U_s \kappa V_s = L_{mi}$. It follows that $U = U_s\sqrt{\kappa}$.
- Eigenvalue Decomposition. This decomposition results in $L_{mi} = U_e \Sigma U_e' = (U_e\sqrt{\Sigma})(\sqrt{\Sigma}U_e')$, where U_e is a matrix of the system's eigenvectors and the diagonal matrix Σ contains the system's eigenvalues. This is very similar to the SVD, and the resulting U matrix is defined as $U = U_e\sqrt{\Sigma}$.

This is simulating the situation where the V matrices cannot be intuited from the system as it is too complicated and has a large number of DOFs.

Table 2 shows the difference in the Euclidian Norm of the UU^T Location Matrix for each of the decomposition techniques ($\Delta_{Lm_{svd}}$ and $\Delta_{Lm_{eig}}$ for SVD and Eignenvalue Decomposition respectively), for each test case, and the original VV^T Location Matrix. The minute differences assert the fact that both decomposition techniques yield the same results. The Eigenvalue decomposition will be used for the rest of the analysis in this paper as it is slightly more simplistic in nature. The equations:

	$\Delta_{Lm_{svd}}$	$\Delta_{Lm_{eig}}$
Test 1	8.04×10^{-16}	0
Test 2	5.86×10^{-14}	7.11×10^{-15}

Table 2: Discrepancies between the norm of the Location Matrices formed by VV^T and UU^T. Δ_{Lm} relates to the type of decomposition technique, and the test number relates to the test cases shown in Equations 34 - 35

$$U_{2_{svd}} = \begin{bmatrix} -0.9922 & 5.1005 \\ 34.6141 & 0.1462 \end{bmatrix}, \tag{36}$$

$$U_{2_{eig}} = \begin{bmatrix} -5.1005 & -0.9922 \\ -0.1462 & 34.6141 \end{bmatrix}, \tag{37}$$

$$L_{m2_{svd}} \approx L_{m2_{eig}} = \begin{bmatrix} 0.0270 & -0.0336 \\ -0.0336 & 1.1982 \end{bmatrix}, \tag{38}$$

show the U matrices for Test, now introducing the fictitious states, and the identical nature of the resulting Location Matrix. Simulation of the two-mass system, with identical inputs, is then performed using the Location Matrix method, with the original inputs, for each U decomposition case, and a variety of $Y(s)$ cases. The resulting identical responses for every $Y(s)$ and decomposition case further consolidates the validity of the Location Matrix method, and eliminates the problems arising with simulating parallel inerter based systems in SIMULINK® due to the presence of algebraic loops. Figure 5 shows the results for Test 2.

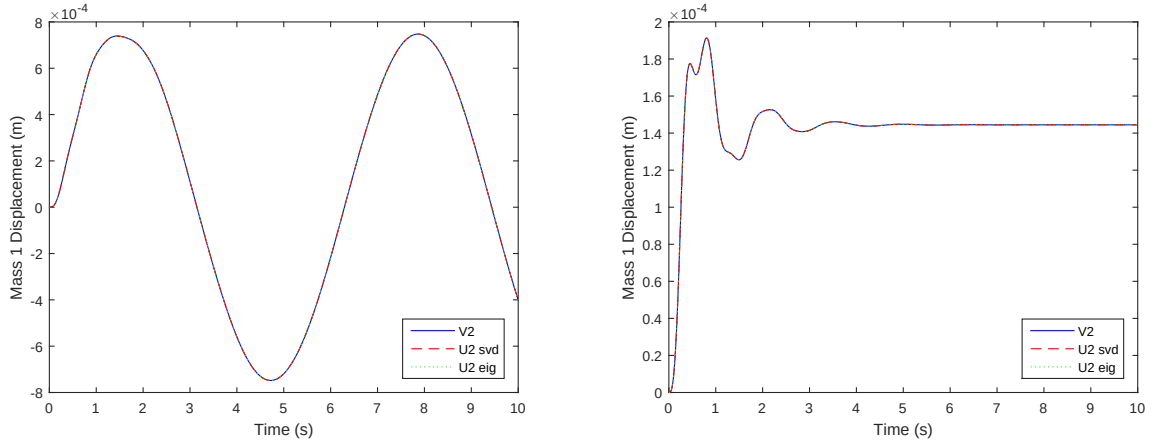

Figure 5: A comparison between the three Location Matrix methods for test case 2 (see Equations 35 - 37) of simulating the simple dynamic system in response to the harmonic input (a), and the step input (b) at mass 1, using an L6 $Y(s)$ layout

4 Application to Railway Vehicle Suspension Optimisation

The Location Matrix method detailed in Section 2 has been used alongside VAMPIRE® to simulate a four-axle railway vehicle [18] with the aim of optimising its lateral suspension and improving its curving performance and passenger comfort. Passenger comfort is quantified by the RMS lateral carbody acceleration when the vehicle is subject to a 5km stretch of lateral track disturbance, taken from a real track. However, to

firstly validate the method on this large railway vehicle model, a simpler input of lateral forcing at the front wheelset in used.

Applying Equation 1 to the railway vehicle, M_0, C_0 and K_0 are respectively the mass, damping and stiffness matrices exported from VAMPIRE® for the hypothetical base model with no primary lateral suspension at all, which amongst other things contain information regarding the wheel-rail contact patch forces. The primary lateral suspension elements are therefore included in the $Y(s)$ part of Equation 1. B includes wheel-rail contact force information when the input $\underline{u}$ matrix consists of real track disturbance data, and is simply unity when $\underline{u}$ is a forcing input. For the forcing input case, $\underline{u}$ is a positive lateral force onj the centre of mass of the front wheelset for the 1st second, an equal and opposite force for the 6th second, and zero at all other times.

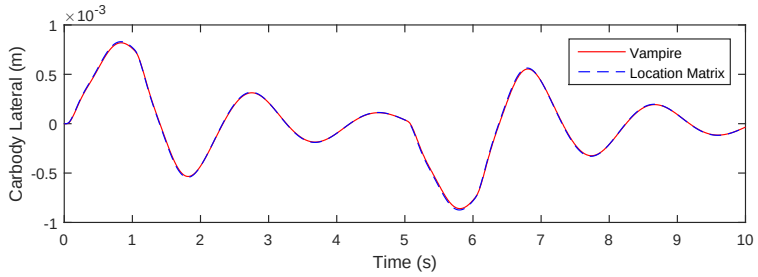

Figure 6: A comparison between the VAMPIRE® and Location Matrix method of simulation, showing the carbody lateral movement with a lateral forcing input of 10kN

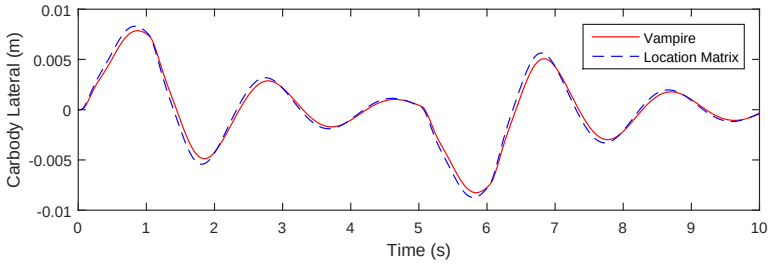

Figure 7: A comparison between the VAMPIRE® and Location Matrix method of simulation, showing the carbody lateral movement with a lateral forcing input of 100kN

Figures 6 and 7 show how the VAMPIRE® and Location Matrix simulations compare for lateral step force magnitudes of respectively 10kN and 100kN, specifically focussing on the carbody's lateral motion, and using an L1 bush layout with default parameter values. It is clear that a closer match occurs at the lower forcing input, and at the higher forcing input the Location Matrix method predicts slightly higher amplitudes of oscillation. It should be noted that at a lateral force of 10kN, many different $Y(s)$ suspension layouts with and without inerters have been tested with the Location Matrix method and the comparisons with VAMPIRE® are correct to a very high degree of accuracy. The transient analysis within VAMPIRE® has been linearised to the extent that there is there is no friction saturation at the contact patch, meaning that a linear contact model is used, however it is impossible to linearise the M_0, C_0 and K_0 matrices completely as the normal force of the vehicle on the track (perpendicular to the wheel's profile) is not distributed equally or consistently when the vehicle is displaced or exhibits hunting motion, resulting in the creep force parameters within the system matrix (Equation 27) varying during the simulation. This cannot be accounted for using the Location Matrix method in its current form as values within the base exported matrices cannot vary, and therefore the time varying normal force is the key factor changing the exported matrices from VAMPIRE® .

Figure 8 demonstrates the extent to which the normal force at the front right wheel contact patch varies

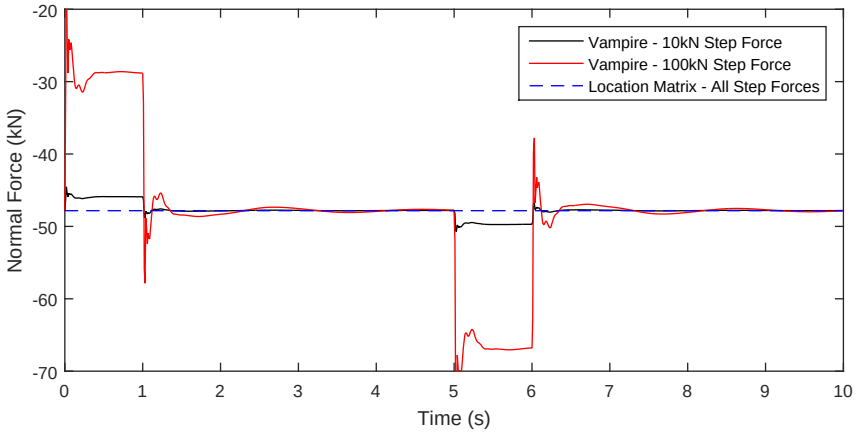

Figure 8: Showing how the normal force at the front left wheel-rail contact patch of the four axle railway vehicle changes during the lateral wheelset 1 step input simulation. Note the vertical (z) direction is defined as positive downwards

during the simulation. When the lateral track displacement is used as the input, and when the stability of the vehicle is assessed using a standard stability track (where the vehicle is excited and then the oscillations are left to die away) comparisons between the VAMPIRE® and Location Matrix methods of calculation yield different results in terms of respectively the RMS lateral acceleration of the carbody, and the steady state displacement of the wheelset.

Although one cannot be certain that the time varying normal force is the only phenomenon which results in a change in the overall system matrix, it can be concluded that although the Location Matrix method can be used to provide preliminary optimisations for a lateral suspension device on a constant normal force and linear contact four axle railway vehicle model, further investigations are required for a full nonlinear analysis. This will most likely come in the form of incorporating VAMPIRE® directly into the MATLAB® optimisation program.

5 Conclusions

This paper has presented and validated a method for simulating and optimising dynamic systems by which interchangeable suspension elements can be incorporated at certain locations via their admittance functions in the Laplace Domain, whilst the base mass, stiffness and damping matrices are used unchanged. This Laplace to state-space Location Matrix method has the potential to allow large scale dynamic systems exported from industrial software to be analysed and chosen suspension networks with admittance functions $Y(s)$ to be optimised for a range of cost functions. The method has been validated using a simple MATLAB® model, and for a range of inerter and non-inerter based suspension networks. When applied to four-axle railway vehicles, a much higher order model, the system responses to small to medium forcing inputs are correct. However, as the inputs and resulting displacements become higher, the system becomes more and more nonlinear, hence changes in base stiffness and damping matrices become significant and can no longer be ignored, therefore the Location Matrix method becomes less effective at simulating responses. This method has potential to produce preliminary optimisations for linearised railway vehicle models and is beneficial to the modelling of any system which includes interchangeable inerter based suspension networks due to its ease of application and the elimination of algebraic loops within SIMULINK® . However, future optimisations of inerter based industrial railway vehicle suspension systems which include all system nonlinearities need to be investigated.

Acknowledgments

The authors would like to thank the EPSRC (Grant References: EP/M507994/1 and EP/P013546/1) and the Royal Society (Grant Reference: IE151194) for funding this research.

References

[1] M. Smith, "Synthesis of mechanical networks: The inerter," *IEEE Transactions on Automatic Control*, vol. 47(10), pp. 1648–1662, 2002.

[2] M. Z. Q. Chen, C. Papageorgiou, F. Scheibe, F.-C. Wang, and M. C. Smith, "The missing mechanical circuit element," *IEEE Circuits and Sytems Magazine*, 2009.

[3] F. Scheibe and M. Smith, "Analytical solutions for optimal ride comfort and tyre grip for passive vehicle suspensions," *Vehicle System Dynamics*, vol. 47(10), pp. 1229–1252, 2009.

[4] S. Evangelou, D. J. N. Limebeer, R. S. Sharp, and M. C. Smith, "An h infinity loop-shaping approach to steering control for high-performance motorcycles," *Lecture Notes in Control and Information Sciences*, vol. 329, pp. 257–275, 2006.

[5] J. Z. Jiang, M. Smith, and N. E. Houghton, "Experimental testing and modelling of a mechanical steering compensator," *International Symposium on Communications, Control and Signal Processing*, pp. 249–254, 2008.

[6] I. F. Lazar, S. A. Neild, and D. J. Wagg, "Using an inerter-based device for structural vibration suppression," *Earthquake Engineering Structural Dynamics*, vol. 43, pp. 1129–1147, 2014.

[7] F.-C. Wang, C.-W. Chen, M.-K. Liao, and M.-F. Hong, "Performance analyses of building suspension control with inerters," *46th IEEE Conference on Decision and Control*, 2007.

[8] S. Y. Zhang, J. Z. Jiang, and S. Neild, "Optimal configurations for a linear vibration suppression device in a multi-storey building," *Structural Control and Health Monitoring*, vol. 24, no. 3, pp. e1887–n/a, 2017. e1887 STC-16-0018.R2.

[9] Y.-C. Chen, S.-Y. Wu, and F.-C. Wang, "Vibration control of a three-leg optical table by mechatronic inerter networks," *SICE Annual Conference 2014*, 2014.

[10] R. Goodall and T. X. Mei, "Mechatronic strategies for controlling railway wheelsets with independently rotating wheels," in *2001 IEEWASME International Conference on Advanced Intelligent Mechatronics Proceedings 6-12 July 2001 Como, Italy*, pp. 225–230, 2001.

[11] T. X. Mei and R. M. Goodall, "Practical strategies for controlling railway wheelsets with independently rotating wheels," *Journal of Dynamic Systems, Measurement, and Control*, vol. 125, pp. 354–360, 203.

[12] T. X. Mei and R. M. Goodall, "Robust control for independently rotating wheelsets on a railway vehicle using practical sensors," *IEEE Transactions on Control Systems Technology*, vol. 9(4), pp. 599–607, 2001.

[13] J. Jiang, T. Mei, and M. Smith, "Curving performance for railway vehicles with advanced passive suspensions," in *23rd International Symposium on Dynamics of Vehicle on Road and Tracks, IAVSD*, 2013.

[14] J. Z. Jiang, A. Z. Matamoros-Sanchez, A. Zolotas, R. M. Goodall, and M. C. Smith, "Passive suspensions for ride quality improvement of two-axle railway vehicles," *IMECHE: Journal of Rail and Rapid Transit*, vol. 229(3), pp. 315–329, 2015.

[15] T. Lewis, J. Jiang, S. Neild, C. Gong, and S. Iwnicki, "Improving ride comfort and trackwear of two-axle railway vehicles using inerter-based lateral suspension layouts," in *Noise and Vibration Emerging Methods, NOVEM*, 2018.

[16] Y. Zhao, G. Tucker, R. Goodall, S. Iwnicki, J. Jiang, and M. Smith, "Developing an inerter model using multibody dynamics software," in *25th International Symposium on Dynamics of Vehicle on Road and Tracks, IAVSD*, 2017.

[17] F. F. Kuo, *Network Analysis and Synthesis*. John Wiley and Sons, 2nd ed., 1962.

[18] RSSB, "Bogiepassenger 39t 15yaw vehicle model, https://www.rssb.co.uk/research-development-and-innovation/research-reports-catalogue/pb009847, accessed 23rd october 2017."